Vitamin D and Calcium Supplementation Accelerates Randall's Plaque Formation in a Murine Model

Elise Bouderlique, Ellie Tang, Joëlle Perez, Amélie E. Coudert, Dominique Bazin, Marie-Christine Verpont, Christophe Duranton, Isabelle Rubera, Jean-Philippe Haymann, Georges Lefthériotis, et al.

Vitamin D and calcium supplementation accelerates Randall's plaque formation in a murine model

Elise Bouderlique,[1,2] Ellie Tang, [1,2] Joëlle Perez [1,2], Amélie Coudert,[3] Dominique Bazin, [4] Marie-Christine Verpont, [1,2] Christophe Duranton,[5] Isabelle Rubera,[5] Jean-Philippe Haymann,[1,2,6] Georges Leftheriotis, [5,7] Ludovic Martin,[8,9] Michel Daudon,[1,2,6] Emmanuel Letavernier,[1,2,6]

[1] Sorbonne Universités, UPMC Univ Paris 06, UMR S 1155, F-75020, Paris, France

[2] INSERM, UMR S 1155, F-75020, Paris, France

[3] UFR d'odontologie (Département des Sciences Biologiques), Université Paris Diderot BIOSCAR - INSERM U1132, Hôpital Lariboisière 75010 PARIS

[4]. Laboratoire de Chimie Physique, CNRS UMR 8000, Université Paris XI, 91405 Orsay, France.

[5] Université Côte d'azur, CNRS-UMR 7370 - Laboratoire de Physiomédecine moléculaire, 06108 Nice, FRANCE

[6] Physiology Unit, AP-HP, Hôpital Tenon, F-75020, Paris, France

[7] Laboratory of Physiology and Molecular Medicine (LP2M), CNRS-UNS UMR 7370, University of Nice, 28 rue de Valombrose, 06107 Nice cedex 2, France

[8] MITOVASC Institute, - UMR CNRS 6015 INSERM U1083 Angers University, France

[9] PXE Reference Center, MAGEC Nord Centerfor rare skin diseases, Angers University Hospital, France

AUTHOR INFORMATION

Correspondence:

Emmanuel LETAVERNIER, Service des Explorations Fonctionnelles Multidisciplinaires, Hôpital TENON, 4 rue de la Chine, 75020 Paris (France). Phone 33 1 56 01 67 73 ; Fax 33 1 56 01 70 03. E-mail: emmanuel.letavernier@aphp.fr

Running Title: Vitamin D and Randall's plaque

Word Count: **2808**

Number of Figures and Tables: Figures: 7; Tables: 2

Keywords: Vitamin D, ABCC6, Kidney stone, Randall's plaque

Disclosures: None declared

Funding statement: This work has been supported by the Agence Nationale de la Recherche (ANR-13-JSV1-0010-01, ANR-12-BS08-0022), the Académie Nationale de Médecine (Nestlé-Waters award), Convergence-UPMC CVG1205 and CORDDIM-2013-COD130042.

38

39

40

Abstract

Most of kidney stones are made of calcium oxalate crystals. Randall's plaque, an apatite deposit at the tip of the renal papilla is considered to be at the origin of these stones. Hypercalciuria may promote Randall's plaque formation and growth.

We analysed whether long-term exposure of Abcc6$^{-/-}$ mice (a murine model of Randall's plaque) to vitamin D supplementation, with or without calcium-rich diet, would accelerate the formation of Randall's plaque. Eight groups of mice (including Abcc6$^{-/-}$ and wild-type) received vitamin D alone (100,000 UI/Kg every 2 weeks), a calcium-enriched diet alone (calcium gluconate 2g/l in drinking water), both vitamin D supplementation and calcium rich diet, or a standard diet (controls) for 6 months. Kidney calcifications were assessed by 3D-micro-computed tomography, µ-Fourier transform infrared spectroscopy, field emission-scanning electron microscopy, transmission electron microscopy and Yasue staining.

At 6 months, Abcc6$^{-/-}$ mice exposed to vitamin D and calcium supplementation developed massive Randall's plaque when compared to control Abcc6$^{-/-}$ mice ($p<0.01$). Wild-type animals did not develop significant calcifications when exposed to vitamin D.

Combined administration of vitamin D and calcium accelerates significantly Randall's plaque formation in a murine model. This original model raises concerns about the cumulative risk of vitamin D supplementation and calcium intakes in Randall's plaque formation.

Introduction

Renal stone incidence is increasing, affecting almost 10% of the population nowadays.[1,2] More than two thirds of all kidney stones are made of calcium oxalate.[3,4] Alexander Randall hypothesized more than eighty years ago that apatite (calcium phosphate) deposits at the tip of renal papilla would initiate stone formation [5] Evan et al. reported that these “Randall's plaque” begin in basement membranes of thin loops of Henle.[6] The same group reported that increased urine calcium excretion could promote Randall’s plaque formation.[7] Stoller et al. and our group evidenced that Randall’s plaque could also originate from vasa recta, capillaries surrounding renal tubules, in the deepest part of the papilla.[8,9] These observations highlight that calcium phosphate supersaturation, predicted to be increased around vasa recta in the papilla, would promote Randall’s plaque formation.[10]

Several recent studies and meta-analyses highlighted that vitamin D and calcium supplementation may increase urine calcium excretion and stone formation, especially in individuals with hypercalciuria.[11,12] A recent randomized controlled trial has shown that the recommended upper serum level of vitamin D, when associated with calcium supplements, results frequently in hypercalciuria.[13] Vitamin D, with or without calcium supplements, is prescribed to prevent bone mass loss, although randomized and controlled studies failed to evidence a protective role of vitamin D against fractures.[14,15] A few reports suggested that kidney stone formers with Randall’s plaques may have an increased biological response to vitamin D but there is little evidence that vitamin D promotes or aggravates Randall’s plaque formation to date.[16]

The combined administration of high calcium intakes and/or vitamin D has been tested in rats, leading to kidney stone formation, defining a model of kidney stone disease.[17] However, rats did not develop tissue calcifications mimicking Randall’s plaques.

More recently, patients affected by pseudoxanthoma elasticum (PXE) have been described to be frequently affected by kidney stones. PXE is a genetic (autosomal recessive) disease due to mutations in *ABCC6* gene. PXE patients are affected by vascular (arterial), retinal and skin calcifications.[18,19] ABCC6 is a transporter expressed in the liver which facilitates the release of extracellular ATP, rapidly converted to inorganic pyrophosphate (PPi) by ectonucleotide pyrophosphatase phosphodiesterase-1 (ENPP1) in vessels. ABCC6 and ENPP1 are actually the main source of systemic pyrophosphate, an inhibitor of calcification limiting ectopic hydroxyapatite (Ca/Pi) crystalline deposits.[20] Patients with PXE, as well as Abcc6$^{-/-}$ mice, have a reduced plasma pyrophosphate level which explains their mineralization disorder.[21,22] PXE patients develop massive Randall's plaques and are prone to develop kidney stones.[23] Interestingly, kidneys from Abcc6$^{-/-}$ mice develop interstitial calcifications with aging (especially after one year), surrounding the loop of Henle and the vasa recta, made of calcium phosphate, and developed in the deepest part of the renal papilla, all features of Randall's plaques.[23] Taken together, these observations suggest pyrophosphate deficiency is a critical determinant of Randall's plaque formation, by increasing calcium phosphate supersaturation in renal papilla.[23]

As Abcc6$^{-/-}$ mice represent a unique model of Randall's plaque, we hypothesized that calcium and/or vitamin D supplementation would accelerate Randall's plaque formation in young Abcc6$^{-/-}$ animals, before the spontaneous development of these papillary calcifications.

Material and Methods

Animal Studies

Mice knock-out for the *Abcc6* gene are usually named Abcc6^{tm1Aabb}. They were produced on a 129/Ola background and then backcrossed into a C57Bl/6J more than 10 times in Professor A. Bergen's laboratory. These mice are designated *Abcc6*$^{-/-}$ in the manuscript.[23]

Fourty-eight 10-weeks old female mice were housed and bred at INSERM UMR S 1155 Mouse Facility, with a twelve-hour dark/light cycle. Mice received standard chow, containing 1000 UI vitaminD3/Kg and 1,05 % calcium ad libitum. Six Abcc6$^{+/+}$ (Wild type-WT) and 6 Abcc6$^{-/-}$ mice had a free access to water containing 80 mg/l of calcium (control group). Six WT and 6 Abcc6$^{-/-}$ mice had a free access to water containing 2g of calcium chloride (calcium group). Considering that a mouse daily drinking intake is about 5 mL/day (C57Bl/6J, 25g), calcium daily intake was 10 mg/mouse/day or 0.4 mg/g/day in “calcium” groups. Six WT and 6 Abcc6$^{-/-}$ mice received vitamin D (ergocalciferol 2500 UI/mouse, Sterogyl 15H, DB Pharma, La Varenne Saint-Hilaire, France) every 2 weeks, e.g 2.5 UI/g/2 weeks, during 6 months by s.c. injection, and had a free access to water containing 80 mg/l of calcium (vitamin D group). Six WT and 6 Abcc6$^{-/-}$ mice received similar vitamin D injections and had a free access to water containing 2g/l of calcium (calcium + vitamin D group).

All studies were performed in accordance with the European Union and National Institutes of Health guidelines (Comité d'Ethique en Experimentation Charles Darwin C2EA-05). The project was authorized by the health ministry and local ethics committee (Authorization number #11420 2017092015335292)

Biological samples and biochemistry

Urine was collected in metabolic cages. Mice had a free access to water (calcium-enriched or not) before the first administration of vitamin D and at 3 and 6 months. Mice were sacrificed 14 days after the last injection of vitamin D and blood was collected at that time.

Several parameters have been measured in urine: diuresis volume, calcium, phosphate, pyrophosphate, creatinine. The blood samples have been analyzed for calcium (total), phosphate, urea and vitamin D (at 6 months).

Urinary creatinine and serum urea, and phosphate levels have been analyzed on IDS-iSYS automat. Calcium serum and urinary levels were measured with the Perkin-Elmer 3300 atomic absorption spectrometer. Vitamin D serum levels have been measured by the IDS-iSYS 25-Hydroxy Vitamin D immunoassay (IS-2700S), to assess 25-Hydroxy Vitamin D (D2 and D3) levels. Pyrophosphate urine levels were measured by using an ATP sulfurylase (M0394, NEB) to convert Pyrophosphate into ATP in the presence of excess of adenosine 5'phosphosulfate (A5508; Sigma Aldrich). Generated ATP was then quantified using the ATP Determination kit (ATPlite 6016941; Perkin Elmer).

X-ray microtomography and 3-dimensional modeling

Left kidneys were fixed in formaldehyde and embedded in paraffin. X-ray CT imaging was performed using a Skyscan 1272 (Bruker, Anvers, Belgium) at Lariboisière Hospital imaging platform (Paris, France). A 6 µm resolution scale was obtained. Shadow images were obtained using an X-ray energy of 65 kV and 150 mA without filter exposition. The angular step between image acquisitions was 0.5° and each image was averaged after 2 frames. Data were reconstructed using Nrecon software (Bruker, Anvers, Belgium) and then exported into a 16-bit Tag Image File Format stack of virtual slices. The Mimics Innovation suite 20.0 (Materialise, Leuven, Belgium) was used for the quantification analysis of papilla's calcification volume, and 3-dimensional modeling of Randall's plaques and kidneys.

Histology and Yasue staining

Kidney tissues were fixed in formaldehyde and embedded in paraffin. Four-µm tissue sections have been performed and stained by Yasue procedure to reveal tissue calcifications.

Field emission-scanning electron microscopy

A Zeiss SUPRA55-VP Field Emission scanning Electron Microscope (Zeiss France, Marly-le-Roi, France) study tissue sections (4 µm), at low voltage (1.4 KeV).

Transmission Electron Microscopy

Half right kidney papilla were fixed in 2.5% glutaraldehyde in 0.1 mmol/L cacodylate buffer (pH 7.4) at 4°C. Fragments were fixed in 1% osmium tetroxide, dehydrated using alcohol series and then embedded in epoxy resin. Semi-thin sections (0.5 µm) were stained using toluidine blue. Ultrastructure sections (80nm) were contrast-enhanced using Uranyl-Less staining. A JEOL 1010 electron microscope (JEOL, Ltd., Tokyo, Japan) with a MegaView III camera (Olympus Soft Imaging Systems GmbH, Munster, Germany) was used to analyze tissues.

µFTIR spectroscopy

Microcalcifications were characterized by using µFourier Transform InfraRed spectrometry (FT-IR) on 4-µm tissue sections deposited on low emission microscope slides (MirrIR, Keveley Technologies, Tienta Sciences, Indianapolis). FT-IR hyperspectral images were analyzed with a Spectrum spotlight 400 FT-IR imaging system (Perkin Elmer Life Sciences, France), at spatial resolution of 6.25 µm and spectral resolution of 8 cm^{-1}. The spectra were recorded in the 4000-700 cm^{-1} mid-InfraRed range.

176

177 **Statistical analyses**

178 Data are expressed as mean (SEM). Data were analyzed with non-parametric tests (Mann-
179 Whitney), using Statview and GraphPad Prism 5.0 softwares (GraphPad Software Inc., San
180 Diego, California).The level of significance was set at <0.05.

181

Results

Serum biochemistry

No significant difference in serum calcium, phosphate and urea levels was observed between the different groups at 6 months (Table 1). An expected but limited rise in vitamin D serum levels (about 1.5×control serum levels) was observed in the groups receiving vitamin D (ergocalciferol) supplementation (Table 1)

Urine biochemistry

Urine calcium, phosphate and pyrophosphate excretion was assessed before treatment, and at 3 and 6 months. No significant difference in urine calcium excretion was observed between WT and Abcc6$^{-/-}$ mice, although there was a systematic trend toward increased urine calcium excretion at 3 and 6 months in animals exposed to vitamin D ± calcium (Table 2). When taken together (considering all Abcc6$^{-/-}$ and WT mice at each time), Abcc6$^{-/-}$ mice had a significantly lower urinary excretion of pyrophosphate in comparison to wild type animals at each time-point (Figure 1, n=24/group, $p<0.01$). When considering subgroups of Abcc6$^{-/-}$ and WT mice, the difference in urine pyrophosphate was inconsistently significant due to the low animal number (n=6/group, Table 2).

Quantification of renal calcification at 6 months

Micro-CT analyses have been performed to assess global kidney calcifications (Figures 2 and 3). Abcc6$^{-/-}$ mice had an increased calcification volume (1443548±174767 µm3) in comparison to control mice (198145±42226 µm3, n=24/group, $p<0.01$). In subgroup analysis, there was a non-significant trend toward an increased renal calcification volume in Abcc6$^{-/-}$ mice exposed to calcium and vitamin D (1939003±484442 µm3) when compared to Abcc6$^{-/-}$ control mice (1051010±166189sem µm3, n=6/group, p=NS, Figure 3).

Micro-CT analyses focused on the kidney papilla have been performed next (Figures 2 and 4). WT animals did not develop significant papillary calcifications, even after 6 months exposure to both calcium and vitamin D (figure 4). Abcc6$^{-/-}$ mice had an increased papillary calcification volume (434910±77943 µm3) in comparison to control mice (62722±23811 µm3, n=24/group, $p<0.01$). In subgroup analysis, there was a significantly increased calcification volume in the renal papilla of Abcc6$^{-/-}$ mice exposed to calcium and vitamin D (892410±172006 µm3) when compared to Abcc6$^{-/-}$ control mice (248937±101734 µm3, n=6/group, $p< 0.01$, Figure 4).

Histopathological analyses and transmission electron microscopy

Yasue staining revealed the presence of rare tubular calcifications (tubular plugs) in WT animals and massive tubular and interstitial calcifications in the renal papilla in Abcc6$^{-/-}$ mice, similar to human Randall's plaque (Figure 5). Of notice, vitamin D and calcium supplementation increased dramatically the interstitial papillary calcified surface in Abcc6$^{-/-}$ mice (Figure 5). Electron microscopy evidenced the massive presence of round-shaped electron-dense structure in the interstitial tissue, around the vasa recta and the loop of Henle, especially in Abcc6$^{-/-}$ mice exposed to calcium and vitamin D (Figure 6).

Field Emission-Scanning Electron Microscopy (FE-SEM) and µFourier Transform InfraRed (µFTIR) spectroscopy

FE-SEM has shown that tubular plugs observed in Abcc6$^{-/-}$ mice exposed to vitamin D and calcium were made of aggregated spherulites (Figure 7A; black arrow) and revealed to a lesser extent the presence of interstitial spherulites embedded in the renal tissue and corresponding to interstitial calcifications (Figure 7A; white arrows). To go further in the characterization of the crystalline phases, we performed µFTIR spectroscopy with an imaging

system. The analysis of the absorption spectrum and its second derivative revealed some features specific for the presence of different absorption bands of the apatite [$Ca_5(PO_4)_3(OH)$], including the ν_3 P-O stretching vibration mode measured at 1035-1045 cm^{-1} (Figures 7B). Carbonate ions were detected together with apatite by their ν_3 C-O stretching vibration mode around 1420 cm^{-1} and the ν_2 C-O bending mode at 875 cm^{-1}. The presence of amorphous calcium phosphate (ACP), revealed by the partial disappearance of the shoulder of the ν_3 P-O absorption band of apatite, has been observed in both interstitial deposits and intratubular calcifications (Figures 7B).

Discussion

The long-term administration of vitamin D, especially in addition to calcium supplementation, accelerates dramatically Randall's plaque formation in Abcc6$^{-/-}$ mice. These 8-mo. old animals were affected by massive papillary calcifications whereas unexposed control Abcc6$^{-/-}$ mice developed tiny interstitial calcifications and tubular plugs. In parallel, wild-type mice exposed to vitamin D, with or without calcium supplementation, developed very sparse tubular calcifications and no Randall's plaque. Abcc6$^{-/-}$ had significantly decreased urinary pyrophosphate levels but calcium and phosphate urine (and serum) levels were similar in wild-type and Abcc6$^{-/-}$ mice. In contrast to our seminal observations, we did not confirm any difference in phosphate metabolism between wild-type and Abcc6$^{-/-}$ mice.[23] Mice exposed to both calcium and vitamin D had a non-significant trend toward higher urine calcium excretion, despite high doses of calcium and vitamin D, in comparison with doses used in humans in clinical practice. It seems difficult to compare calcium homeostasis in mice and humans but the modest increase in vitamin D serum levels, the non-significant increase in urine calcium excretion and the absence of hypercalcemia in animals exposed to calcium and vitamin D rules out the hypothesis of an "intoxication". Nevertheless, in mice affected by pyrophosphate deficiency, even a mild increased in urine calcium excretion was sufficient to accelerate the papillary calcification process.

Interestingly, Sprague Dawley rats exposed to high calcium intake did not develop renal calcifications and rats exposed to vitamin D alone developed hypercalciuria but only tiny calcium phosphate kidney stones.[17] By contrast, the synergistic administration of calcium and vitamin D promoted the development of large stones but no Randall's plaque. The genetic hypercalciuric stone-forming rat (GHS) have an increased expression of the vitamin D receptor (VDR) in intestine, bone, and kidney.[24] These animals develop calcium phosphate

kidney stones but, again, no Randall's plaque. It appears therefore that vitamin D, especially in combination to calcium is not sufficient to induce papillary calcifications, whose initiation may be due to calcification inhibitors defect, but accelerates dramatically the development of the Randall's plaque in Abcc6$^{-/-}$ mice.

Predisposed individuals may be at risk to form kidney stones when exposed to vitamin D, especially when vitamin D and calcium intakes are combined. In the Women Health Initiative (WHI) study, a controlled randomized study, 36,282 postmenopausal women received 1 gram calcium and 400IU vitamin D daily or a placebo during 7 years.[11] The treatment did not reduce significantly bone fractures but an increased kidney stone risk has been described in women who received calcium and vitamin D. Recent studies confirmed that vitamin D, especially when prescribed in addition to calcium supplementation, increases significantly urine calcium excretion and in some studies the risk to develop kidney stones.[12,13] By contrast, some studies did not identify an increased risk of kidney stone after exposure to vitamin D alone (without calcium supplementation) during a median follow-up of 3.3 years.[25] Interventional studies remain sparse but recent observations show that some kidney stone formers may develop hypercalciuria after vitamin D "repletion".[26,27] An important point to take into consideration is the time required to develop Randall's plaque, which precede stone formation. Actually, vitamin D increases urine calcium excretion, which may accelerate plaque formation and promote calcium oxalate stone formation several years later.[7] The situation may have worsened during the past decades because of the increase in vitamin D prescription, although there is no evidence that vitamin D supplementation may protect against fractures or other conditions, including cancers, cardiac and vascular diseases, obesity, diabetes, depression, falls, infectious diseases and maternal/perinatal conditions.[28] Interestingly, Ferraro et al. analysed the association of vitamin D intakes and the risk to develop kidney stones and found no association in the Health Professionals Follow-up Study

and Nurses' Health Study I but an increased risk in the more recent Nurses' Health Study II, including women receiving an increased amount of vitamin D supplements.[29]

We observed a synergistic effect of combined vitamin D/calcium supplementation in experimental models, consistent with clinical studies. Of note, calcium intake in the absence of vitamin D did not increase the risk Randall's plaque formation in our in murine model but also in humans: on the contrary, higher dietary calcium is associated with a lower risk to develop kidney stones.[30] This results from calcium-oxalate complex formation in the intestine, limiting oxalate absorption and eventually calcium oxalate stone formation.

Our results raise concerns about the prescription of vitamin D and calcium to patients affected by PXE. We recently described the presence of massive Randall's plaque and frequent kidney stones in these patients and it may be hypothesized that vitamin D prescription could accelerate plaque and stone formation in patients affected by pyrophosphate deficiency.[23] A deficiency in urine pyrophosphate has been reported in kidney stone formers but pyrophosphate level in urine is difficult to assess in routine practice. This explains probably why few studies focused on the importance of pyrophosphate in kidney stone formation, and no study highlighted its role in Randall's plaque formation until recently.[31-33]

Most of kidney stones are made of calcium oxalate and many of them originate from Randall's plaque. Some observations suggested that patients affected by Randall's plaque could be more "sensitive" to vitamin D.[16] The dramatic acceleration of papillary calcifications by the combined administration of vitamin D and calcium in Abcc6$^{-/-}$ mice suggests that in some genetically predisposed individuals, combined calcium and vitamin D intake could in theory accelerate Randall's plaque formation, deserving specific clinical studies to address this concern.

Acknowledgements

The authors thank Liliane Louedec and Claude Kitou for their excellent advice on mouse care and management.

Authors contribution

EL, EB, and MD designed the study
EB, ET, JP, AC, DB, MCV, CD, IR, JPH, GL, LM, MD, VP, JZ, OLS, MD, and EL carried out experiments and clinical research
EB, ET, JP,AC,DB,CD, IR, MD and EL analyzed the data
EB, ET, and EL made the figures
EB, ET, JP, AC, DB, CD, IR, MD, and EL drafted and revised the paper

EL is the guarantor of this work and, as such, had full access to all of the data in the study and takes responsability for the integrity of the data and the accuracy of the data analysis

All authors approved the final version of the manuscript

Financial Conflict of Interest: none

References

1. Stamatelou KK, Francis ME, Jones CA, Nyberg LM, Curhan GC: Time trends in reported prevalence of kidney stones in the United States: 1976-1994. Kidney Int 2003; 63: 1817-1823

2. Ziemba JB, Matlaga BR: Epidemiology and economics of nephrolithiasis. Investig Clin Urol 2017; 58: 299-306

3. Daudon M, Doré JC, Jungers P, Lacour B: Changes in stone composition according to age and gender of patients: a multivariate epidemiological approach. Urol Res 2004; 32: 241-247

4. Singh P, Enders FT, Vaughan LE, Bergstralh EJ, Knoedler JJ, Krambeck AE, Lieske JC, Rule AD: Stone Composition Among First-Time Symptomatic Kidney Stone Formers in the Community. Mayo Clin Proc 2015; 90: 1356-1365

5. Randall A: The origin and growth of renal calculi. Ann Surg 1937; 105: 1009-1027

6. Evan AP, Lingeman JE, Coe FL, Parks JH, Bledsoe SB, Shao Y, Sommer AJ, Paterson RF, Kuo RL, Grynpas M: Randall's plaque of patients with nephrolithiasis begins in basement membranes of thin loops of Henle. J Clin Invest 2003; 111: 607-616

7. Kuo RL, Lingeman JE, Evan AP, Paterson RF, Parks JH, Bledsoe SB, Munch LC, Coe FL: Urine calcium and volume predict coverage of renal papilla by Randall's plaque. Kidney Int 2003; 64: 2150-2154

8. Stoller ML, Low RK, Shami GS, McCormick VD, Kerschmann RL: High resolution radiography of cadaveric kidneys: unraveling the mystery of Randall's plaque formation. J Urol 1996; 156:1263-1266

9. Verrier C, Bazin D, Huguet L, Stéphan O, Gloter A, Verpont MC, Frochot V, Haymann JP, Brocheriou I, Traxer O, Daudon M, Letavernier E: Topography, Composition and Structure of Incipient Randall Plaque at the Nanoscale Level. J Urol 2016, 196: 1566-1574

10. Tournus M, Seguin N, Perthame B, Thomas SR, Edwards A: A model of calcium transport along the rat nephron. Am J Physiol Renal Physiol 2013, 305: F979-994

11. Jackson RD, LaCroix AZ, Gass M, Wallace RB, Robbins J, Lewis CE, Bassford T, Beresford SA, Black HR, Blanchette P, Bonds DE, Brunner RL, Brzyski RG, Caan B, Cauley JA, Chlebowski RT, Cummings SR, Granek I, Hays J, Heiss G, Hendrix SL, Howard BV, Hsia J, Hubbell FA, Johnson KC, Judd H, Kotchen JM, Kuller LH, Langer RD, Lasser NL, Limacher MC, Ludlam S, Manson JE, Margolis KL, McGowan J, Ockene JK, O'Sullivan MJ, Phillips L, Prentice RL, Sarto GE, Stefanick ML, Van Horn L, Wactawski-Wende J, Whitlock E, Anderson GL, Assaf AR, Barad D; Women's Health Initiative Investigators: Calcium plus vitamin D supplementation and the risk of fractures. N Engl J Med 2006, 354: 669-683

12. Hu H, Zhang J, Lu Y, Zhang Z, Qin B, Gao H, Wang Y, Zhu J, Wang Q, Zhu Y, Xun Y, Wang S: Association between Circulating Vitamin D Level and Urolithiasis: A Systematic Review and Meta-Analysis. Nutrients 2017, 9: E301

13. Aloia JF, Katumuluwa S, Stolberg A, Usera G, Mikhail M, Hoofnagle AN, Islam S. Safety of calcium and vitamin D supplements, a randomized controlled trial. Clin Endocrinol (Oxf) 2018, 89: 742-749

14. Bolland MJ, Grey A, Avenell A: Effects of vitamin D supplementation on musculoskeletal health: a systematic review, meta-analysis, and trial sequential analysis. Lancet Diabetes Endocrinol 2018, 6: 847–858

15. Reid IR, Bolland MJ, Grey A. Effects of vitamin D supplements on bone mineral density: a systematic review and meta-analysis. The Lancet 2014, 383: 146–155

16. Letavernier E, Vandermeersch S, Traxer O, Tligui M, Baud L, Ronco P, Haymann JP, Daudon M: Demographics and characterization of 10,282 Randall plaque-related kidney stones: a new epidemic? Medicine (Baltimore) 2015, 94: e566

17. Letavernier E, Verrier C, Goussard F, Perez J, Huguet L, Haymann JP, Baud L, Bazin D, Daudon M: Calcium and vitamin D have a synergistic role in a rat model of kidney stone disease. Kidney Int 2016, 90: 809-817

18. Li Q, Jiang Q, Pfendner E, Váradi A, Uitto J: Pseudoxanthoma elasticum: clinical phenotypes, molecular genetics and putative pathomechanisms. Exp Dermatol 2009, 18: 1-11

19. Le Saux O, Urban Z, Tschuch C, Csiszar K, Bacchelli B, Quaglino D, Pasquali-Ronchetti I, Pope FM, Richards A, Terry S, Bercovitch L, de Paepe A, Boyd CD: Mutations in a gene encoding an ABC transporter cause pseudoxanthoma elasticum. Nat Genet 2000, 25: 223-227

20. Jansen RS, Duijst S, Mahakena S, Sommer D, Szeri F, Váradi A, Plomp A, Bergen AA, Oude Elferink RP, Borst P, van de Wetering K: ABCC6-mediated ATP secretion by the liver is the main source of the mineralization inhibitor inorganic pyrophosphate in the systemic circulation-brief report. Arterioscler Thromb Vasc Biol 2014, 34: 1985-1989

21. Vanakker OM, Leroy BP, Coucke P, Bercovitch LG, Uitto J, Viljoen D, Terry SF, Van Acker P, Matthys D, Loeys B, De Paepe A: Novel clinico-molecular insights in pseudoxanthoma elasticum provide an efficient molecular screening method and a comprehensive diagnostic flowchart. Hum Mutat 2008, 29: 205

22. Ziegler SG, Ferreira CR, MacFarlane EG, Riddle RC, Tomlinson RE, Chew EY, Martin L, Ma CT, Sergienko E, Pinkerton AB, Millán JL, Gahl WA, Dietz HC: Ectopic calcification in pseudoxanthoma elasticum responds to inhibition of tissue-nonspecific alkaline phosphatase. Sci Transl Med 2017, 9: 393

23. Letavernier E, Kauffenstein G, Huguet L, Navasiolava N, Bouderlique E, Tang E, Delaitre L, Bazin D, de Frutos M, Gay C, Perez J, Verpont MC, Haymann JP, Pomozi V, Zoll J, Le Saux O, Daudon M, Leftheriotis G, Martin L: ABCC6 Deficiency Promotes Development of Randall Plaque. J Am Soc Nephrol 2018, 29: 2337-2347

24. Bushinsky DA, Frick KK, Nehrke K: Genetic hypercalciuric stone-forming rats. Curr. Opin. Nephrol. Hypertens 2006, 15: 403–418

25. Malihi Z, Lawes CMM, Wu Z, Huang Y, Waayer D, Toop L, Khaw KT, Camargo CA, Scragg R: Monthly high-dose vitamin D supplementation does not increase kidney stone risk or serum calcium: results from a randomized controlled trial. Am J Clin Nutr 2019, in press

26. Johri N, Jaeger P, Ferraro PM, Shavit L, Nair D, Robertson WG, Gambaro G, Unwin RJ. Vitamin D deficiency is prevalent among idiopathic stone formers, but does correction pose any risk? Urolithiasis 2017, 45: 535-543

27. Vitale C, Tricerri A, Bermond F, Fabbrini L, Guiotto C, Marangella M: Metabolic effects of Cholecalciferol supplementation in kidney stone formers with vitamin D deficiency. G Ital Nefrol 2018, 35

28. Autier P, Mullie P, Macacu A, Dragomir M, Boniol M, Coppens K, Pizot C, Boniol M: Effect of vitamin D supplementation on non-skeletal disorders: a systematic review of meta-analyses and randomised trials. Lancet Diabetes Endocrinol 2017, 5: 986-1004

29. Ferraro PM, Taylor EN, Gambaro G, Curhan GC: Vitamin D Intake and the Risk of Incident Kidney Stones. J Urol 2017, 197: 405-410

30. Taylor EN, Curhan GC: Dietary calcium from dairy and nondairy sources, and risk of symptomatic kidney stones. J. Urol 2013, 190: 1255–1259

31. Roberts NB, Dutton J, Helliwell T, Rothwell PJ, Kavanagh JP: Pyrophosphate in synovial fluid and urine and its relationship to urinary risk factors for stone disease. Ann Clin Biochem 1992, 29: 529-534

32. Sharma S, Vaidyanathan S, Thind SK, Nath R: Urinary excretion of inorganic pyrophosphate by normal subjects and patients with renal calculi in north-western India and the effect of diclofenac sodium upon urinary excretion of pyrophosphate in stone formers. Urol Int 1992, 48: 404-408

33. Simonet BM, Grases F, March JG: Enzymatic determination of pyrophosphate in urine by flow methods. Anal Sci 2003, 19: 1029-1032

Figure Legends

Figure 1. Urinary pyrophosphate excretion at baseline, 3 and 6 months.

Urine pyrophosphate excretion, indexed to urine creatinine (µmol/mmol) was significantly decreased in Abcc6 $^{-/-}$mice in comparison to WT animals (*: $p < 0.05$, n=24 animals/group).

Figure 2. Renal calcifications assessment by X-Ray tomography

Micro-CT analyses allowed the identification of kidney calcifications. The global volume of the calcifications (in red) has been assessed after 3D kidney reconstruction (Figure 2A-H).

WT mice (Figure 2 A-D) did not develop significant calcifications, whereas

Abcc6 $^{-/-}$ mice (Figure 2E-H) developed calcifications, especially at the tip of the papilla

(A) WT Control; (B) WT Calcium; (C) WT Vitamin D ; (D) WT Calcium + Vitamin D; (E) Abcc6$^{-/-}$ Control; (F) Abcc6$^{-/-}$ Calcium; (G) Abcc6$^{-/-}$ Vitamin D; (H) Abcc6 $^{-/-}$ Calcium + Vitamin D

Figure 3. Renal calcification global volume

The global volume of the calcifications has been quantified (μm^3) after 3D kidney reconstruction. Global renal calcification volume was significantly increased in Abcc6 $^{-/-}$ mice in comparison to WT animals but there was no significant difference among Abcc6$^{-/-}$ mice subgroups (n=6/group).

Figure 4. Papillary calcifications

The volume of the calcifications has been quantified (μm^3) in each papilla after 3D kidney reconstruction. Global papillary calcification volume was significantly increased in Abcc6 $^{-/-}$ mice exposed to both calcium and vitamin D vs Abcc6 $^{-/-}$ control mice (*: $p < 0.05$, n= 6 animals/group).

Figure 5. Characterization of papillary calcifications: Yasue staining

Yasue staining revealed intratubular and interstitial calcifications predominating in the renal papilla. WT mice developed very sparse and rare tubular plugs, even after exposure to calcium and vitamin D (Figure 5A-D magnification x100). By contrast, Abcc6 $^{-/-}$ mice developed papillary calcifications (tubular plugs and interstitial calcifications, mimicking the human Randall's plaque, Figure 5E-H). The exposure to vitamin D, especially in addition to calcium increased interstitial calcifications (Figure 5G-H).

(A) WT Control; (B) WT Calcium; (C) WT Vitamin D ; (D) WT Calcium + Vitamin D; (E) Abcc6$^{-/-}$ Control; (F) Abcc6$^{-/-}$ Calcium; (G) Abcc6$^{-/-}$ Vitamin D; (H) Abcc6 $^{-/-}$ Calcium + Vitamin D

Figure 6. Characterization of papillary calcifications: transmission electron microscopy.

Transmission electron microscopy evidenced that the interstitial deposits observed in Abcc6^{-} /- mice exposed to vitamin D were round-shaped, concentric and electron-dense structure, surrounding vasa recta and loop of Henle, features similar to the incipient Randall's plaque observed in humans.

Figure 7. Characterization of papillary calcifications: Field emission-scanning electron microscopy images and Fourier Transform InfraRed spectroscopy.

Field emission-scanning electron microscopy images showed tubular plug structure (black arrow), and to a lesser extent interstitial deposits (Figure 7A, white arrows). Calcifications were made of spherulite aggregates, a typical feature of calcium phosphate (apatite) deposits. These deposits were made of apatite and to a lower extent amorphous carbonated calcium phosphate as evidenced by FTIR spectroscopic imaging analyses (Figure 7B: typical spectrum of a mixture of apatite and amorphous calcium phosphate and Fourier transform infraRed microspectroscopy hyperspectral image of a papilla from a Abcc6$^{-/-}$exposed to calcium and vitamin D).

Table 1 : Serum biological parameters

	WT				**Abcc6$^{-/-}$**			
	Control	Calcium	Vitamin D	Calcium + Vitamin D	Control	Calcium	Vitamin D	Calcium + Vitamin D
Urea mmol/l	9.34 ±±0.55	10.78 ± 0.51	9.40 ± 0.21	10.12 ± 0.43	10.67 ± 1.80	9.59 ± 0.37	8.72 ± 0.59	8.32 ± 0.38
Calcium mmol/l	2.51 ± 0.1	2.53 ± 0.07	2.23 ± 0.08	2.49 ± 0.11	2.49 ± 0.06	2.65 ± 0.15	2.5 ± 0.06	2.4 ± 0.1
Phosphate mmol/l	1.83 ± 0.06	2.16 ± 0.39	1.83 ± 0.18	2.38 ± 0.25	2.73 ± 0.41	1.94 ± 0.08	2.29 ± 0.14	2.29 ± 0.08
Vitamin D ng/ml	82.5 ± 6.6	87.6 ± 6.9	123.4 ± 6.9*	144.8 ± 14.5*	88.9 ± 6.9	74.9 ± 3.0	124.4 ± 5.8*	114 ± 5.9*

* p<0.05 versus control and calcium group

Table 2 : Urine biological parameters

	WT				**Abcc6$^{-/-}$**			
	Control	Calcium	Vitamin D	Calcium + Vitamin D	Control	Calcium	Vitamin D	Calcium + Vitamin D
At baseline								
Calcium/creatinine mmol/mmol	0.97 ± 0.23	0.66 ± 0.09	0.59 ± 0.06	0.71 ± 0.06	1.06 ± 0.15	1.02 ± 0.11	0.99 ± 0.2	1.23 ± 0.31
Phosphate/creatinine mmol/mmol	15.5 ± 3.3	16.5 ± 1.5	19.6 ± 2.2	24 ± 2.5	23.2 ± 4.6	14.7 ± 1.3	17.4 ± 1.1	20.3 ± 3.2
Pyrophosphate/creatinine µmol/mmol	1.89 ± 0.32	3.84 ± 0.79	2.71 ± 0.46	2.96 ± 0.57	1.82 ± 0.3	1.85 ± 0.4	1.86 ± 0.15	1.42 ± 0.42
At 3 months								
Calcium/creatinine mmol/mmol	0.87 ± 0.08	0.70 ± 0.11	0.94 ± 0.11	0.85 ± 0.09	0.84 ± 0.09	0.89 ± 0.19	1.08 ± 0.13	1.06 ± 0.15
Phosphate/creatinine mmol/mmol	14.6 ± 1.6	15.2 ± 1.5	16.9 ± 1.8	12.6 ± 0.5	16.1 ± 0.8	9.3 ± 1.5	13.7 ± 2.1	17.1 ± 1.8
Pyrophosphate/creatinine µmol/mmol	2.8 ± 0.36	3.25 ± 0.19	2.62 ± 0.3	2.76 ± 0.26	1.83 ± 0.36	1.9 ± 0.41	1.8 ± 0.29	2.68 ± 0.66
At 6 months								
Calcium/creatinine mmol/mmol	0.77 ± 0.17	0.71 ± 0.13	1.03 ± 0.24	0.91 ± 0.12	0.76± 0.11	0.63 ± 0.03	1.06 ± 0.1	0.93 ± 0.06
Phosphate/creatinine mmol/mmol	14.3 ± 0.2	13.1 ± 1	17.8 ± 1.9	18.8 ± 2.1	16 ± 0.9	13.3 ± 1.1	13.2 ± 0.9	14.8 ± 0.7
Pyrophosphate/creatinine µmol/mmol	3.92 ± 0.43	3.26 ± 0.47	3.3 ± 0.28	3.17 ± 0.58	2.68 ± 0.43	3.01 ± 0.41	1.83 ± 0.18	2.32 ± 0.5

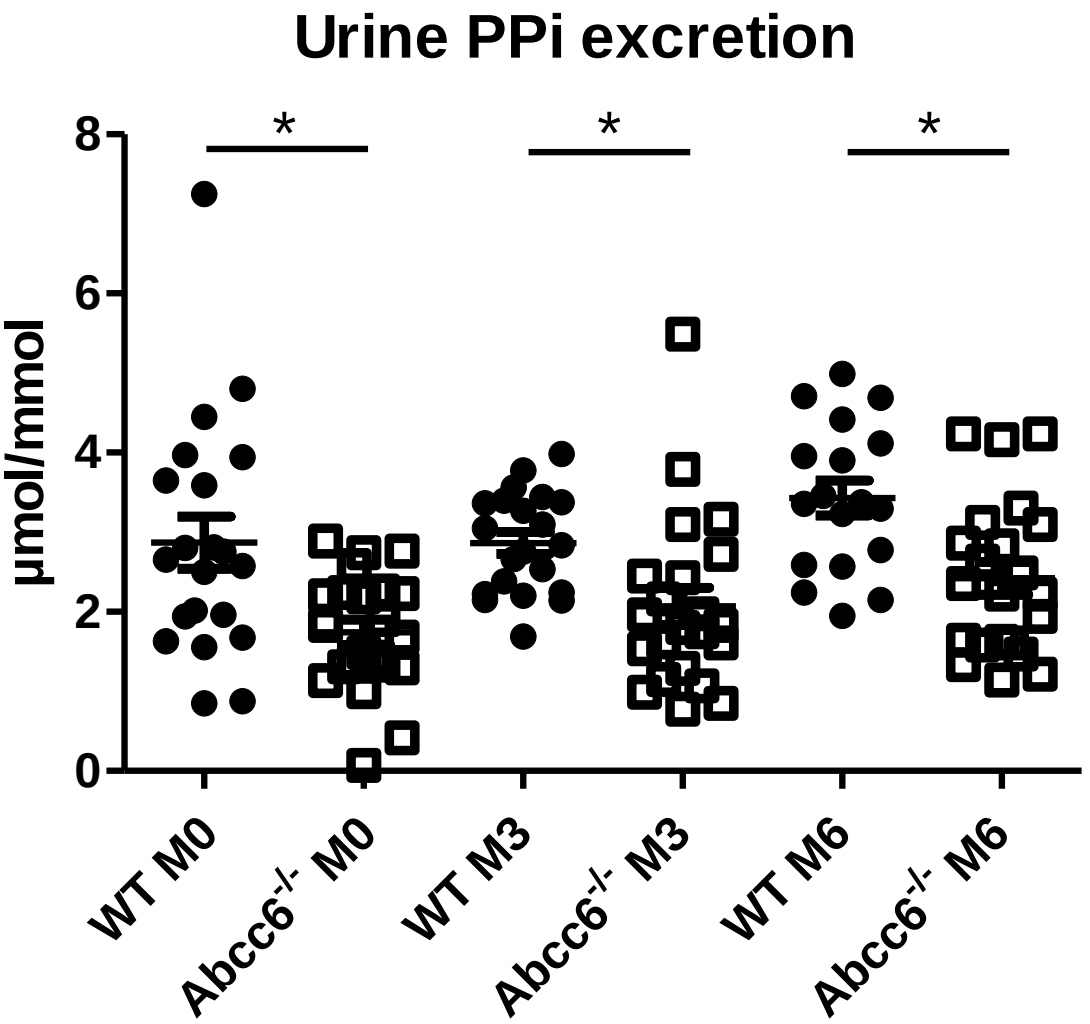
Urine PPi excretion
µmol/mmol
8
6
4
2
0
*
*
*
WT M0
Abcc6-/- M0
WT M3
Abcc6-/- M3
WT M6
Abcc6-/- M6

A
WT control
B
WT calcium
C
WT Vit D
D
WT calcium+ VitD
E
Abcc6-/- control
F
Abcc6-/- calcium
G
Abcc6-/- VitD
H
Abcc6-/- calcium+ VitD

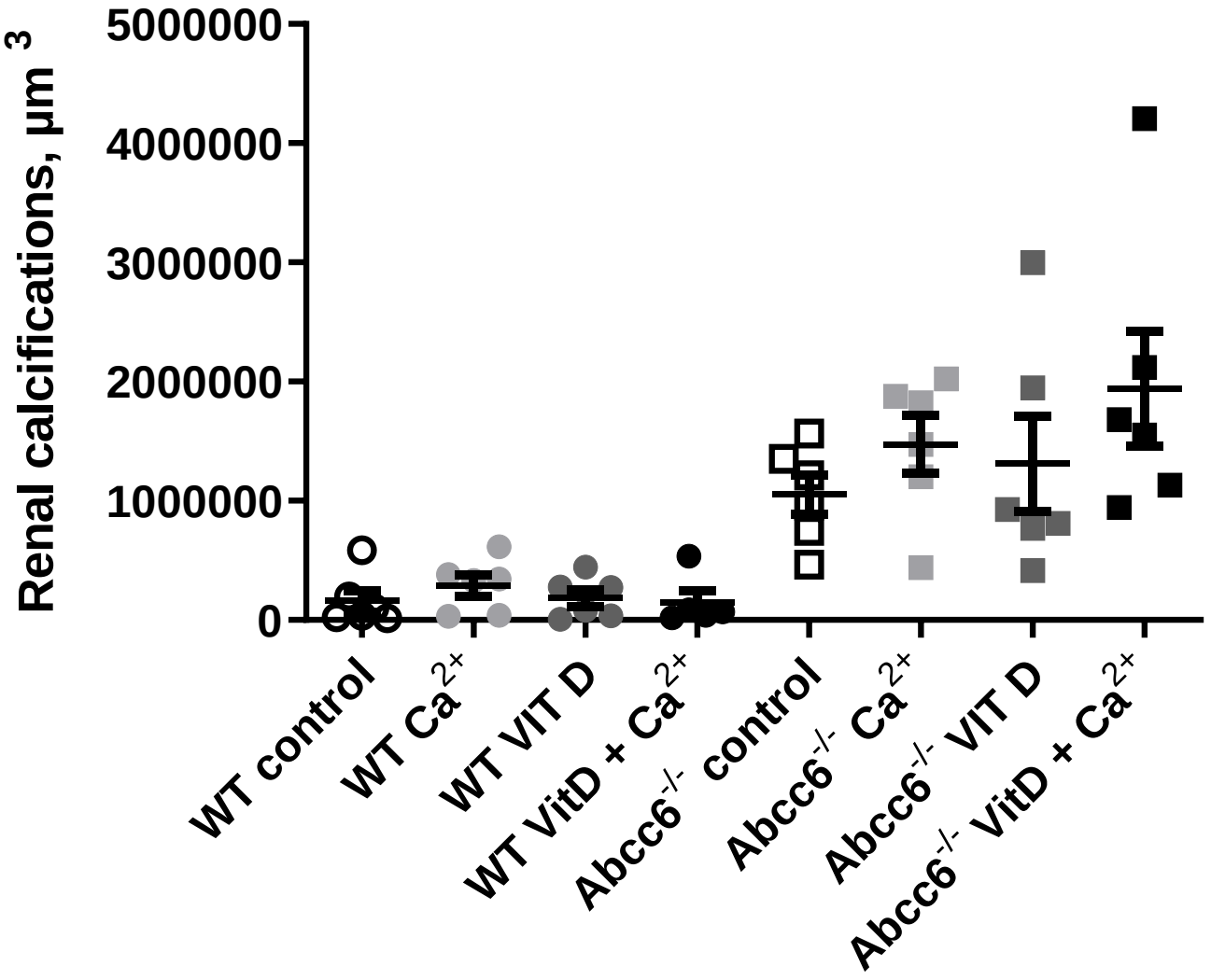
Renal calcifications, µm 3
5000000
4000000
3000000
2000000
1000000
0
WT control
WT Ca2+
WT VIT D
WT VitD + Ca2+
Abcc6-/- control
Abcc6-/- Ca2+
Abcc6-/- VIT D
Abcc6-/- VitD + Ca2+

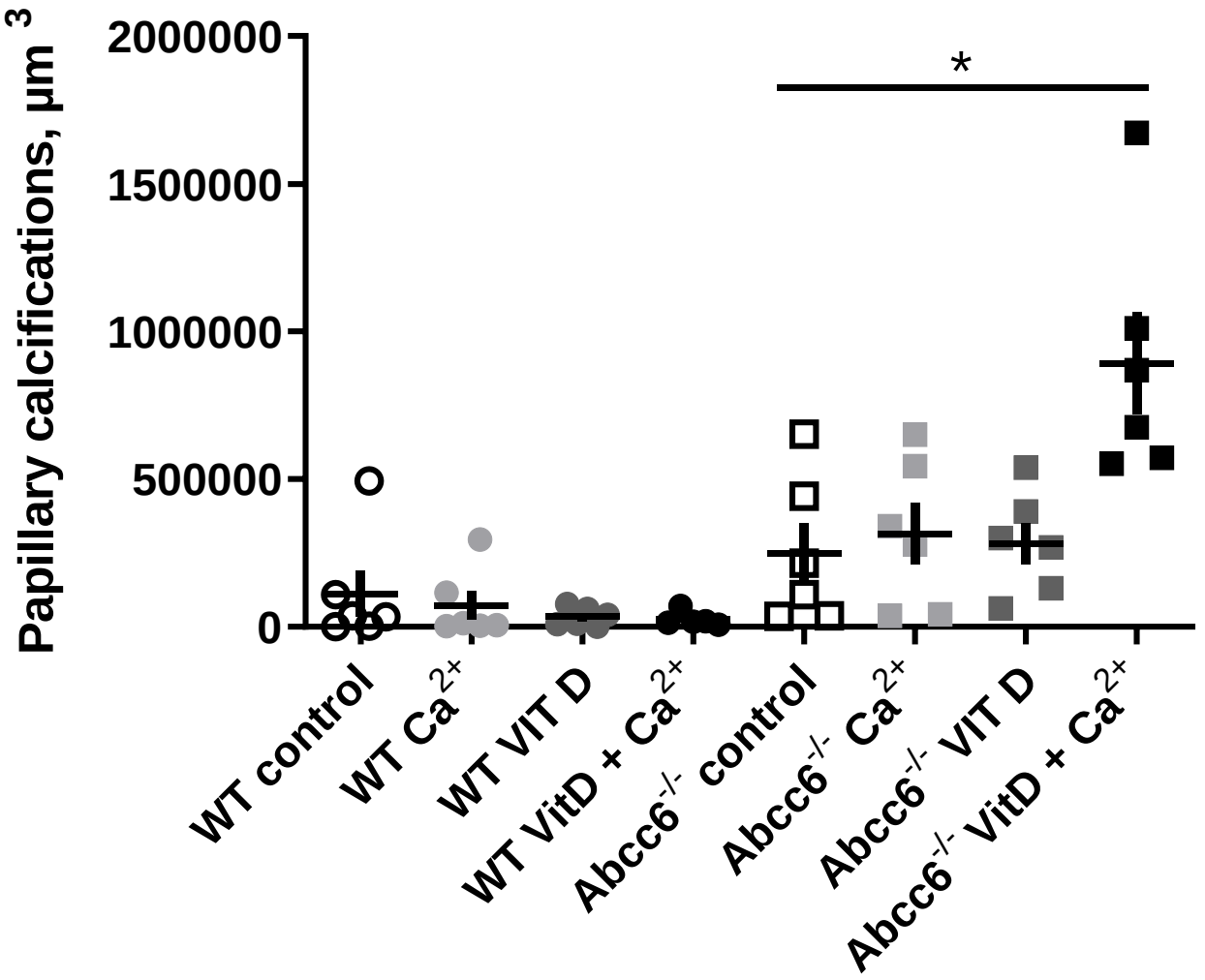
Papillary calcifications, µm3
2000000
1500000
1000000
500000
0
*
WT control
WT Ca2+
WT VIT D
WT VitD + Ca2+
Abcc6-/- control
Abcc6-/- Ca2+
Abcc6-/- VIT D
Abcc6-/- VitD + Ca2+

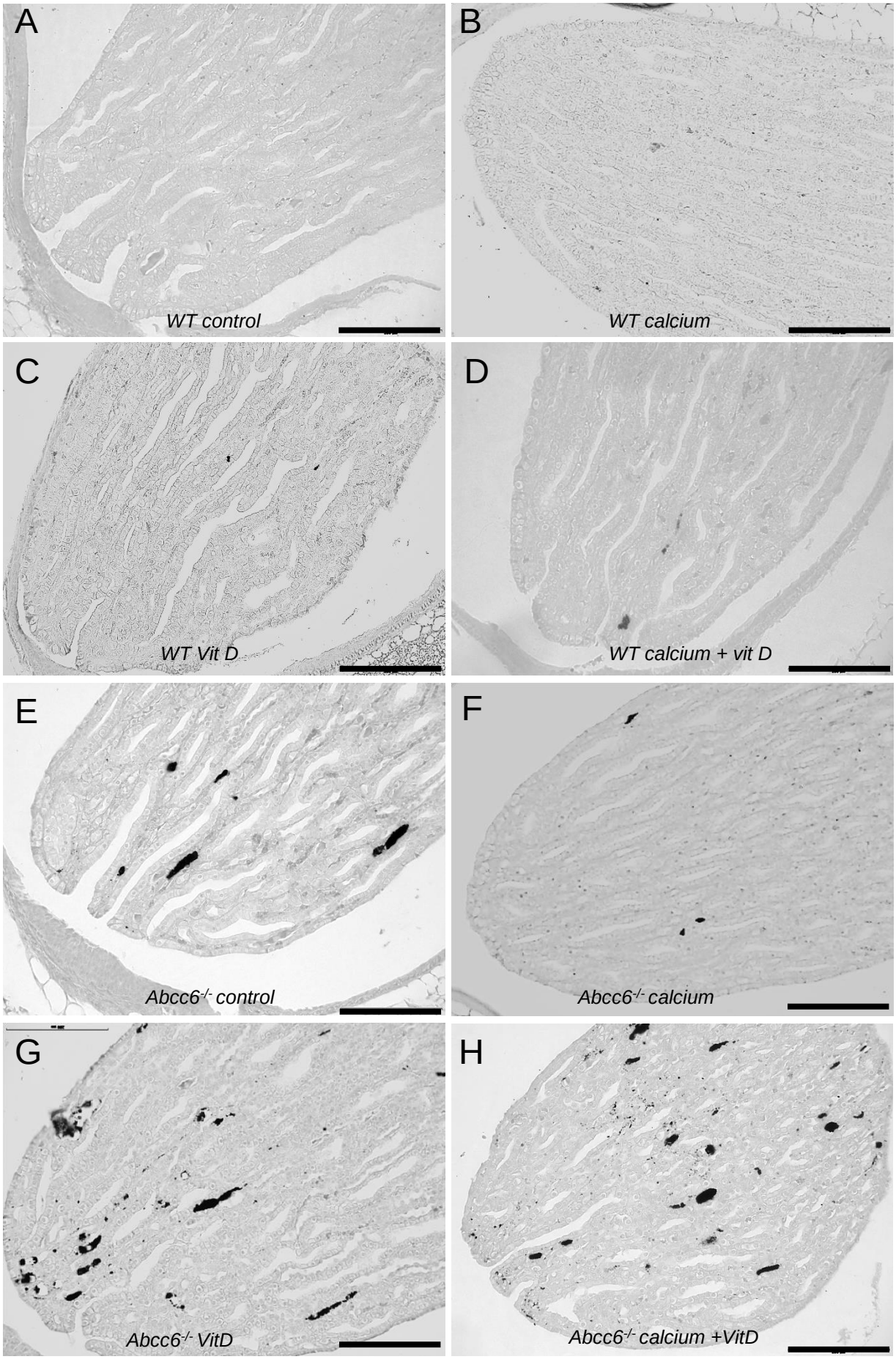
A
WT control
B
WT calcium
C
WT Vit D
D
WT calcium + vit D
E
Abcc6-/- control
F
Abcc6-/- calcium
G
Abcc6-/- VitD
H
Abcc6-/- calcium +VitD

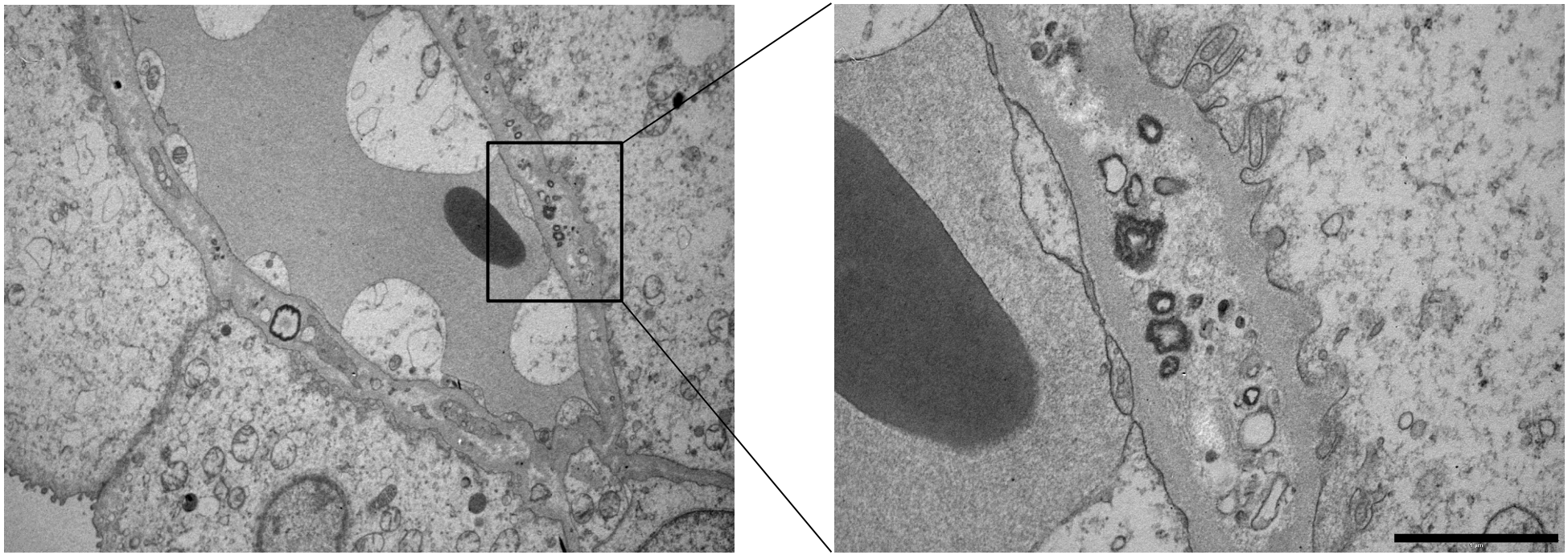

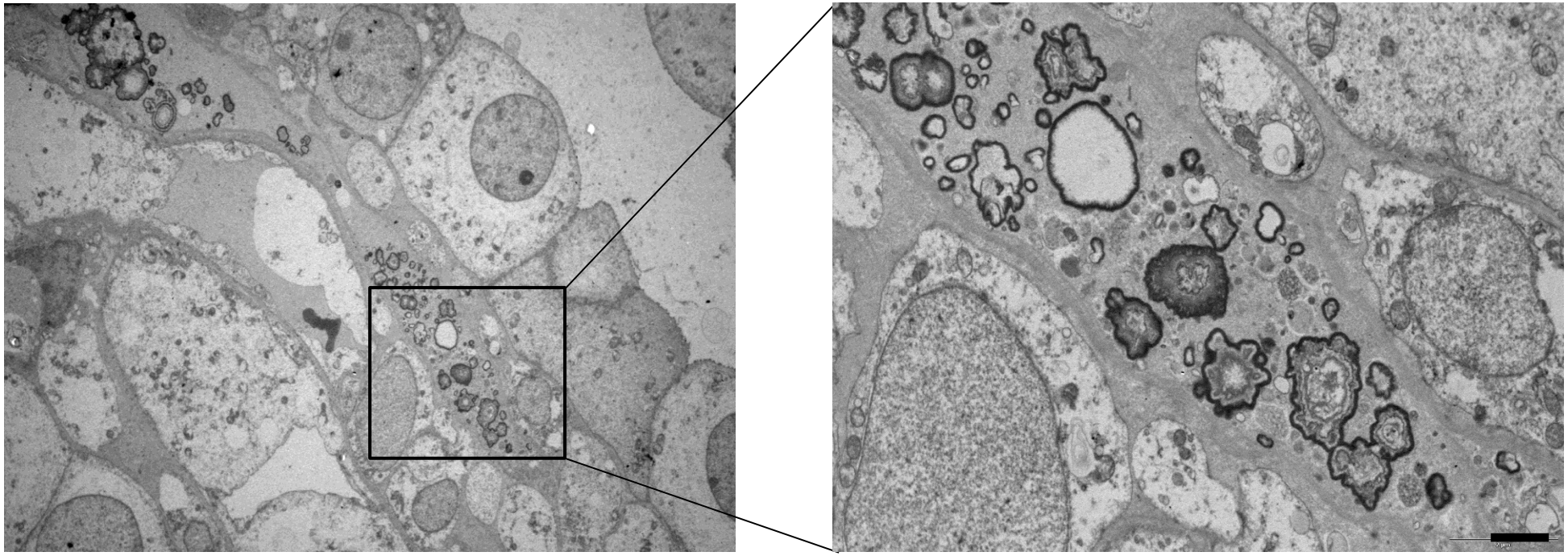

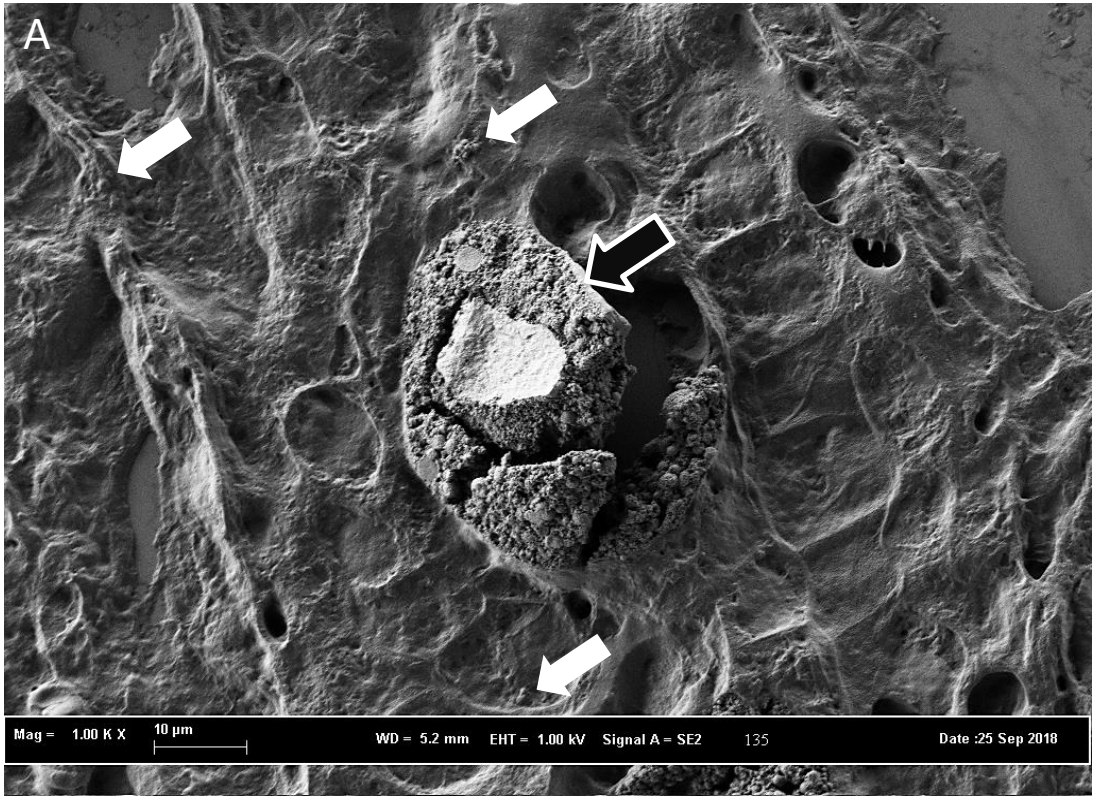
A
Mag = 1.00 K X
10 µm
WD = 5.2 mm
EHT = 1.00 kV
Signal A = SE2
135
Date :25 Sep 2018

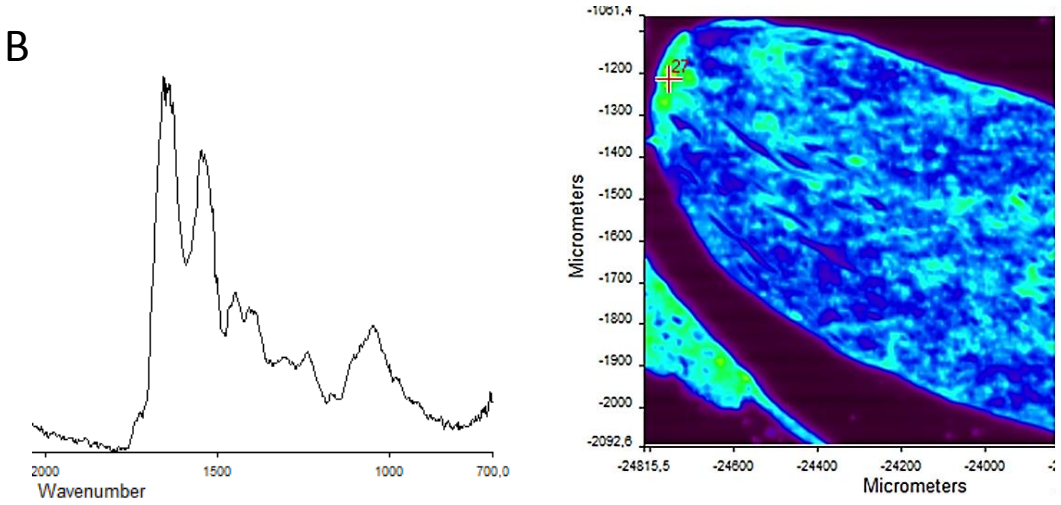
B
2000
1500
1000
700,0
Wavenumber
-1061,4
-1200
-1300
-1400
-1500
-1600
-1700
-1800
-1900
-2000
-2092,6
Micrometers
-24815,5
-24600
-24400
-24200
-24000
Micrometers